Hydromorphological Classification Using Synchronous Pressure and Inertial Sensing

Asko Ristolainen, Kaia Kalev, Jeffrey Andrew Tuhtan, Alar Kuusik, and Maarja Kruusmaa

***Abstract*— Classification of river morphology is often based on hydromorphological units (HMUs) identified from field measurements. Established survey methods rely on expert judgment or collection of field point measurements. When used for HMU classification, these methods can suffer from high errors due to the variations in the sampling environment, causing low repeatability. In order to expedite field data collection and increase HMU classification accuracy, we propose a multisensory device, the hydromast. Each hydromast provides a new source of data to classify HMUs. The modules are inexpensive and highly portable, consisting of a synchronous array of commodity pressure and inertial sensors. Rapid, local changes in the flow field are recorded with absolute and differential pressure sensors. At the same time, slower depth-integrated flow signals are obtained from a small damped cylindrical mast, driven by vortex-induced vibrations. In contrast to existing passive flow measurement technologies, the hydromast uses fluid–body interactions to provide flow measurements. This allows for minimal signal processing and simple feature extraction. An array of three hydromasts was used to collect ten samples in three river HMUs with shallow depths and highly turbulent flows with smooth and rough beds. We investigated classification accuracy using single, dual, and triple hydromast arrays with pressure, inertial, and combined features using linear regression, a genetic algorithm, and a neural network. Although limited in scope, the set of spot measurements covering three HMUs showed that a single multimodal sensor could deliver an overall classification accuracy of 89% of the HMUs, and an increase of up to 99% was achieved using a multimodal triple hydromast array. These preliminary results show promise in using hydromasts for rapid and robust HMU classification, providing a new way to collect and assess river survey data.**

***Index Terms*— Fluid flow measurements, hydrologic measurements, water.**

I. Introduction

HYDROMORPHOLOGICAL units (HMUs) are river sections broken down into a series of multiscale elements, and should ideally include both field and remote sensing data [1]. The reach scale divides the river longitudinally into a series of subunits, and is the most commonly investigated type of HMU as it contains salient features of the ecological–geomorphological interface [2]. Remote sensing can be used to efficiently collect spatial data and quantify temporal effects [3]. However, HMU classification still requires *in situ* measurements to supply ground truth data [4]. Once HMUs are classified, they provide essential geospatial information for end users including regional planning, flood control, and biodiversity assessment [5]–[7].

Current river morphological survey methodologies rely heavily on expert opinion [8]. This sets limits on the automated classification of HMUs, primarily due to a lack of repeatable field data collection and assessment methods [9]. In general, the local variables such as depth, velocity, cover type, and bed surface condition are used as the primary features to first classify HMUs, which can then be related to aquatic habitats [10], [11]. More recently, local variables such as river surface flow speed have been measured remotely with different technologies [12]–[16].

Hauer *et al.* [17] found functional linkages between the flow velocity, depth, and bottom shear stress, and developed relations to ecological mesohabitat units using LiDAR bathymetry and 2-D hydrodynamic models. A hydromorphological index of diversity using the coefficient of variation of the velocity and water depth has also been applied using extensive field data and hydrodynamic models to evaluate reach-scale heterogeneity in alpine gravel-bed streams [18]. In addition, a time-series study of reach-scale units has shown that the classification boundaries can merge or shift depending on the river flow rate [19]. Due to the spatial and temporal changes occurring in rivers, it is, therefore, key that objective and repeatable field measurement of the local variables serve as inputs to calibrate and validate HMU classification methods. This requires the repeated collection of field data corresponding to different flow rates which are caused by seasonal changes in the runoff.

At the reach scale, data collection of the local variables is expensive and time consuming. This is because a plurality of separate point measurements (depth, time-averaged velocity, and sediment samples) must be collected separately and processed before classification can be performed. The hydromast, a simple, timesaving, field survey device that collects local flow information using collocated synchronous pressure and inertial data, provides a methodology to collect an ensemble of relevant hydrodynamic data at each measurement

Manuscript received April 10, 2017; revised August 21, 2017 and November 21, 2017; accepted January 2, 2018. Date of publication February 9, 2018; date of current version May 21, 2018. This work was supported by the European Union's Horizon 2020 Research and Innovation Program under Grant 635568 through the frame of Lakhsmi Project. The work of J. A. Tuhtan was supported in part by the Estonian Base Financing under Grant B53, in part by Octavo and PUT under Grant 1690, and in part by Bioinspired flow sensing. *(Corresponding author: Asko Ristolainen.)*

A. Ristolainen, K. Kalev, J. A. Tuhtan, M. Kruusmaa are with the Centre for Biorobotics, Tallinn University of Technology, 12618 Tallinn, Estonia (e-mail: asko.ristolainen@ttu.ee).

A. Kuusik is with the Thomas Johann Seebeck Department of Electronics, Tallinn University of Technology, 12618 Tallinn, Estonia.

This paper has supplementary downloadable material available at http://ieeexplore.ieee.org, provided by the author.

Color versions of one or more of the figures in this paper are available online at http://ieeexplore.ieee.org.

Digital Object Identifier 10.1109/TGRS.2018.2795641

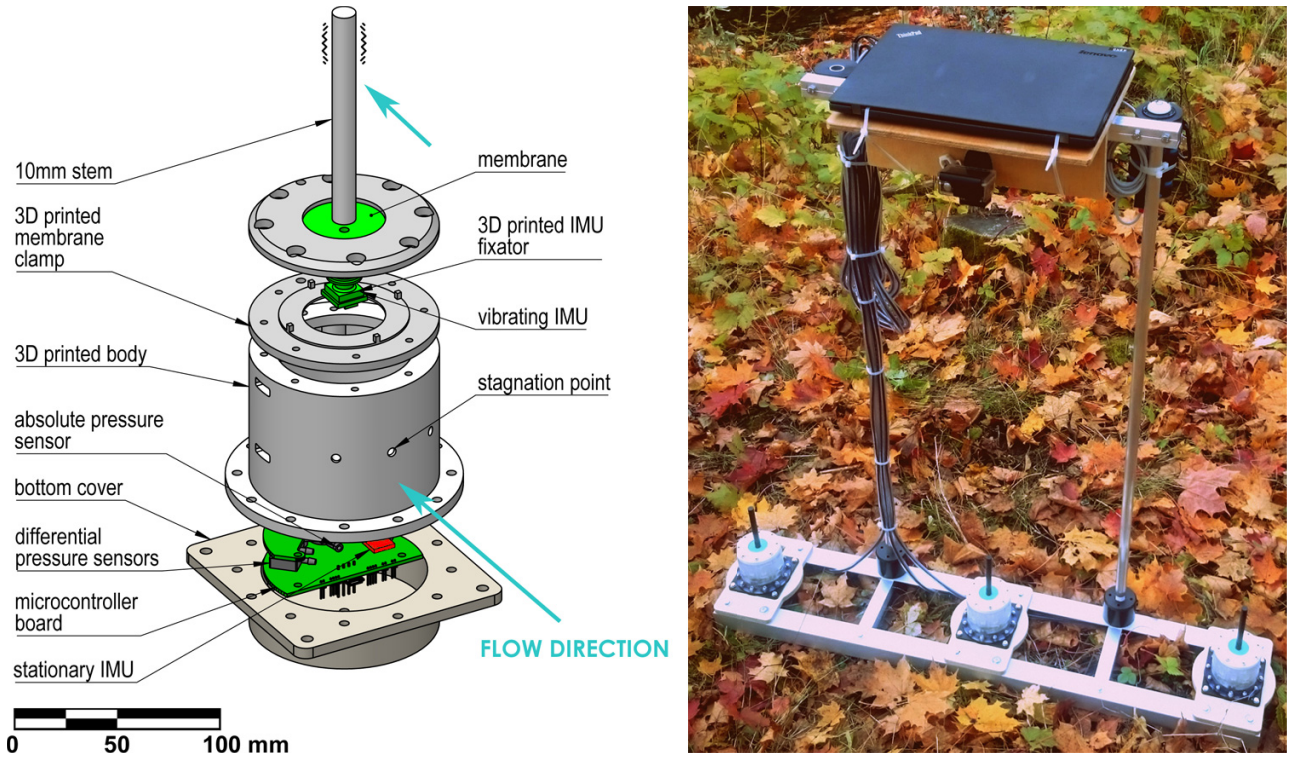

Fig. 1. (Left) Pressure-inertial hydromast breakdown. (Right) Field setup with triple hydromast array.

location. Thus, the time reduced is at least 1/3, and in the case that classification is implemented *in situ*, even more time can be saved.

Increasingly, unmanned aerial systems are beginning to provide a rapid and inexpensive way to collect imagery with a ground sample distance of < 0.5 m [20], suitable for HMU classification and analysis. However, there still exists a significant gap in available field survey methods capable of obtaining repeatable validation data for reach-scale HMU classification. In order to fill this gap, we developed the hydromast to simultaneously collect an ensemble of relevant hydrodynamic variables for HMU validation.

II. Methods

A. Sensor Description

The hydromast was inspired by the multimodal mechanoreceptive flow sensing organs of fish. It is an upscaled version of the biological neuromast, consisting of a vibrating stem elastically fixed to a pressure sensing cylindrical body (Fig. 1). The bulk flow velocity drives the stem vibration, as the random forcing due to turbulence tends to cancel itself out [21]. Furthermore, the stem integrates hydrodynamic interactions over its height. The stem motion is registered with a custom design micromechanical inertial measuring unit (IMU) fixed to its lower end. We have shown that this design can accurately estimate the bulk flow speed under steady flows [22]. A 100-mm-long, 10-mm-diameter rigid POM plastic stem provided a suitable combination of size and density for flow sensing in rivers in the range of 0–1 m/s, with a sensitivity of 0.1 m/s or for flow velocities < 0.5 and 0.05 m/s for velocities > 0.5 and up to 1 m/s. These sensitivities are primarily a function of the membrane stiffness and stem's properties (mass, length, and diameter) and can be tuned to different ranges of mean flow velocities. Considering the flows in lowland rivers typical to Northern Europe, the range of 0–1 m/s was chosen for the hydromasts investigated in this paper. The noise introduced by vibrations of the hydromast body was partially compensated by adding a secondary IMU to the body.

In addition to the inertial-sensing stem, an absolute pressure sensor was added to record the water depth (MPX5100GP, NXP) accompanied by two differential sensors (MPXV5004DP, NXP) to estimate the dynamic pressure changes at the stagnation point facing into the bulk flow measured between the center point and side points. This differential sensor design was chosen as it was proven successful for rapid flow speed estimation [23]. The complete design of the pressure-inertial hydromast is shown in Fig. 1. The total cost of components, assembly, and testing for a three-unit hydromast array is estimated at e 2000.

B. Sensor Calibration

All pressure sensors were calibrated in a static water tank. One port of the pressure sensor was connected to a tube, which was then lowered into the tank for ten different water depths. The relationship between the observed pressure (Pa) and the pressure sensor output voltage (mV) was recorded at each depth 10 times per sensor, and correction equations for the depth were obtained. The relations were found to be linear with R^2 values shown in Table I.

Stem calibration followed the procedure outlined in [22]. The mast reaction to the bulk flow speed was found with the hydromast fixed in the middle of a flow tunnel with a working

TABLE I
HYDROMAST PRESSURE CALIBRATION R^2 VALUES

Hydromast	Left differential pressure sensor R^2 value	Right differential pressure sensor R^2 value	Absolute pressure sensor R^2 value
1	0.9826	0.9865	0.9699
2	0.9937	0.9918	0.9838
3	0.9949	0.9987	0.9942

TABLE II
SITE SAMPLING SUMMARY

Site	Geographic location	Average flow speed [m/s] (STD)	Average depth [m] (STD)	Water temperature [24]	Air temperature [24] [°C]	HMU class*
1	59°23'42.8"N 24°17'40.2"E	0.326 (0.066)	0.333 (0.050)	4.3	4.8	Glide
2	59°23'44.9"N 24°17'40.0"E	0.487 (0.233)	0.299 (0.052)	3.1	4.1	Rapid
3	59°24'05.5"N 24°16'55.2"E	0.306 (0.112)	0.352 (0.077)	1.1	2.5	Riffle

*Classification made based on definitions from Paraciewicz [10]

section of 0.5 m × 0.5 m × 1.5 m. The experiments used flow speeds up to 0.5 m/s (increments of 0.1 m/s) and the mean power spectral densities of the stems were related to the flow speed. Before the field experiments, the IMUs were calibrated using their internal self-calibration firmware, which requires only that the devices were kept still before being inserted into the water.

C. Study Sites

Field experiments were conducted in the Keila River in Northern Estonia, near the Keila Waterfall (59° 23′ 45.9″N 24° 17′ 47.1″E, WGS 84, Fig. 2). A discharge of 1.75 m^3/s (with flow speeds shown in Table II) was recorded at the Keila River gauging station (59° 18′ 31.0″N 24° 26′ 05.0″E) during the days (October 17, 2016–October 21, 2016) when the field experiments were conducted. Each of the three sites corresponds to a different HMU following the classification structure suggested by Parasiewicz [10]. Ten spot measurement locations were chosen at each site. Because the three sites have overlapped range of depths and velocities, they also represent a case where a collection of point measurements would be difficult to correctly classify the HMUs. Site 1 was classified as a glide, located directly upstream from the Keila Waterfall. Here, the riverbed consists predominantly of a horizontal limestone slab with little aquatic vegetation. It has a flat water surface with nearly uniform flow. Site 2, a rapid, was located immediately downstream of the waterfall. At this site, the riverbed consisted of cobbles, inducing large turbulent eddies within the water column. Site 3, classified as a riffle, was close to the mouth of the river and some measurement locations were observed to have a smooth bed and water surface similar to Site 1, at other locations with small stones and cobbles, combined with aquatic vegetation induced local turbulence similar to that found at Site 2. Surface and underwater imagery at typical spot measurement locations for each of the three sites are shown in Fig. 3.

At each site, the ten spot measurement locations were distributed over the left, center, and right channel sections, all with similar depth and flow conditions. At Site 2, the chosen locations were limited by the large cobble substrate, as it was necessary to find a suitable bed location for the three-sensor array.

A propeller current meter (MFP126-S, GEOPACKS, Hatherleigh, U.K.) was used to record ten velocity measurements 50 mm in front of each hydromast's mast in the array, at approximately the mid-mast height. The time-averaged flow velocity from all locations for each site is provided in Table II. The experiments were conducted within one week with no rainfall in the area. The water temperature in the area decreased over time due to the frost at nights.

D. Experimental Setup

The three hydromasts were mounted on a CNC cut plywood base with an aluminum laptop mount. The center-to-center distance between the hydromasts was 0.45 m. The hydromasts

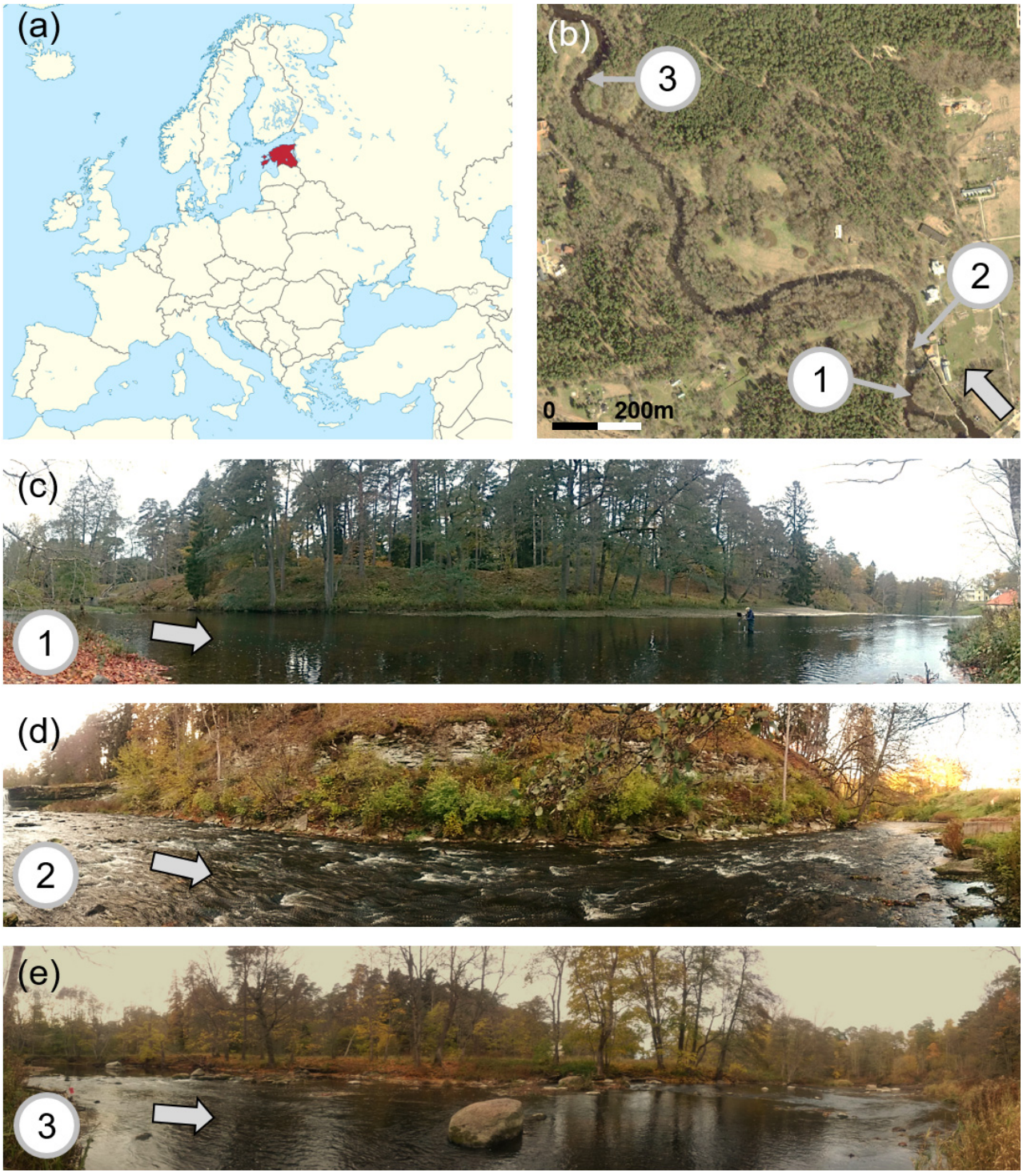

Fig. 2. Overview of the three HMU field sites at the Keila River, Estonia. (a) Map of Europe with Estonia shown in red. (b) Site locations overlaid on an orthoimage. (c) Site 1, glide. (d) Site 2, rapid. (e) Site 3, riffle. Arrows indicate flow direction, and (c)–(e) are not to scale.

were numbered 1–3, beginning from the leftmost hydromast perpendicular to the flow. The rig supported a laptop, USB hub (DUB-H7, D-Link, Taiwan), external power source (Outdoor PowerBank 10.05, Wentronic GmbH Germany), and GoPro Hero 3 camera (GoPro Inc., USA) to monitor the stem movements from above. A bubble spirit level was installed to observe and correct the array during measurement (Fig. 1).

All hydromasts were visually inspected and cleaned of debris before measurement. The hydromasts were synchronized by simultaneously resetting the timestamp counter in the microcontrollers. At each spot measurement location,

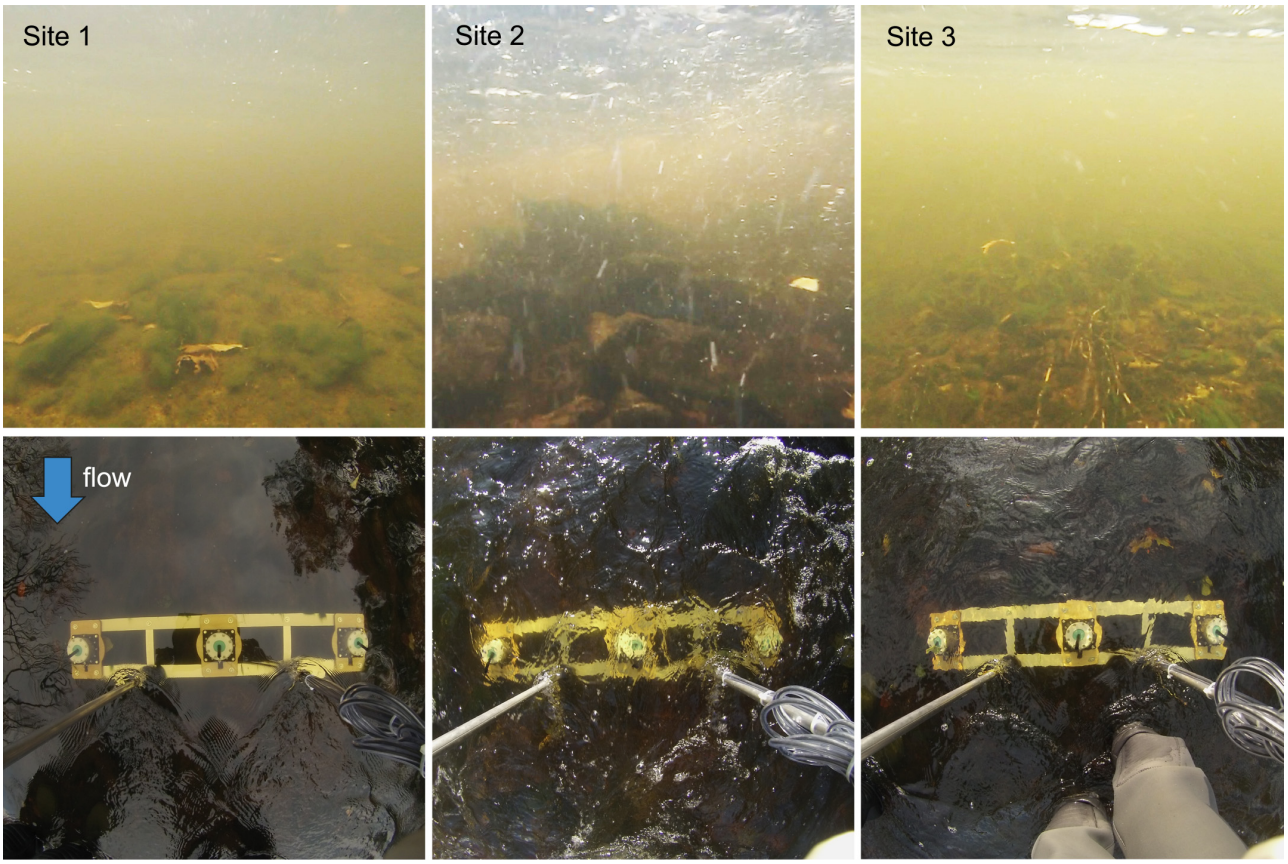

Fig. 3. (Top) Underwater and (Bottom) elevation view of typical spot measurement locations at each of the three field sites.

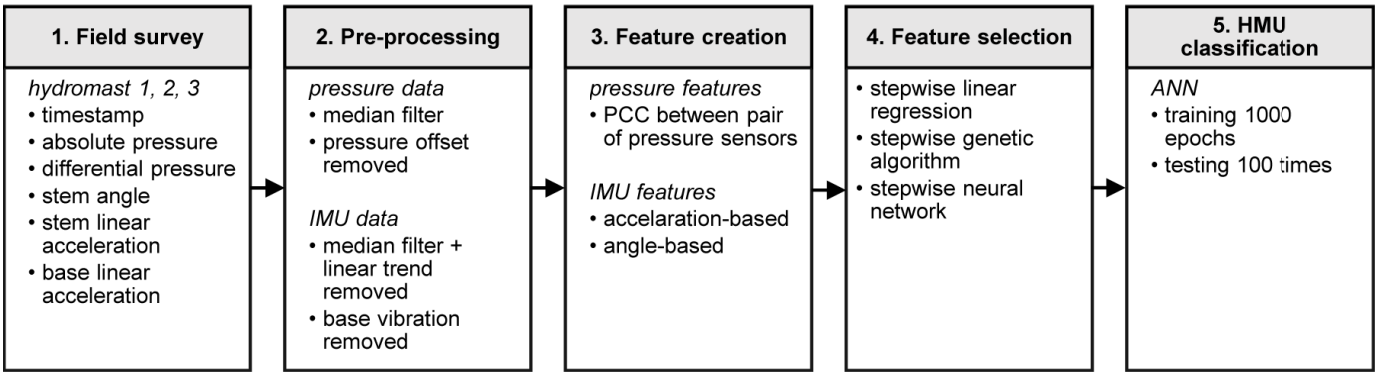

Fig. 4. HMU classification workflow.

measurement data were recorded for 90 s to laptop using TeraTerm serial port access software. Sampling rates for both IMUs and pressure sensors were 100 Hz. A short video clip at each spot measurement location was recorded above the sensors for 15 s.

E. Data Analysis and Site Classification

The overview of the data analysis and HMU classification broken down into five steps is summarized in Fig. 4. First, field data were obtained using the synchronized array. Second, the signals were preprocessed using a median filter with additional offsets removed from pressure data and base vibrations removed from the IMU data. As a third step, features were calculated for pressure and IMU data. Pearson product moment coefficients (ρ) between all possible pressure sensor pairs were found. Acceleration and angle features were created from the IMU sensor data. Before classification, feature selection was performed using stepwise linear regression, a genetic algorithm, and an artificial neural network (ANN).

It is important to note that because we are using an array of hydromasts and each unit records a collection of pressure and inertial data, there exists a very large dimensional space which can be populated with physical predictors. The "features" that are used can be combinations of the predictors (as is the case

using the product moment correlation), as well as particular statistical metrics of individual predictors (such as the mean and median). It is for this reason that we have included step 4, "Feature selection" into the classification workflow. The feature selection step goes through the large, initial set of possible features and selects out only those which have the highest utility. Afterward, the HMU was classified using an ANN. MATLAB 2015 software was used for the entire HMU classification process.

F. Data Preprocessing

The IMU and pressure sensor data preprocessed using a median filter with a window size of 4. In order to reduce the background noise caused by sensor vibrations, the hydromast body accelerations recorded by the stationary IMU were subtracted from the stem IMU. Offset correction for each pressure sensor was performed by setting the differential pressure (DP) sensor readings to 0 mV under no-flow conditions.

1) Pressure Sensor Data: Data fusion was used to investigate if the classification performance could be improved by combining the information from two or more pressure sensors [25]. The first step in data fusion is to investigate the similarity between sensor pairs [26]. The Pearson product moment coefficient (ρ) [27] was chosen for the pressure sensors, as it has previously been successfully applied for pressure-based flow velocity estimation [28]. In this paper, ρ values between all pressure sensors were calculated and saved into the feature vector PS for the later HMU classification, where PS1 is the ρ value between hydromast 1 right DP and total pressure (TP) sensors and PS36 is ρ value between hydromast 3 TP and left DP sensors. A detailed description of all the features investigated in this paper is provided in the supplementary material.

2) IMU Data: The linear accelerometer and angle data from the IMU were found to be highly periodic. Therefore, ρ-based sensor fusion was not a suitable option for the IMU data. For example, two identical sine waves with a phase shift of 90° would have a ρ value of 0, even though they are identical. Therefore, additional features for the hydromast IMU data were required.

First, the linear accelerometer's dominant frequency and its amplitude were calculated. This is the frequency which carried the maximum energy among all frequencies in the spectrum [29]. The dominant frequency was determined using the normalized fast Fourier transform to calculate the amplitude spectrum. The frequency component with the highest peak was taken as the dominant frequency.

Next, features based on a 1/3 octave band analysis were generated. This method was chosen because it was more efficient than analyzing the spectrum on frequency-by-frequency basis and will not lead to *ad hoc* frequency band selection. The frequency range was divided into six sets of 1/3 octave bands with corresponding center frequencies 12.5, 16, 20, 25, 31.5, and 50 Hz, and the power in each frequency range was calculated [30]. The linear accelerometer data were used to generate features using the mean, median (more stable considering outliers than the mean), energy, kurtosis, skewness, entropy, average autocorrelation zero-crossing time Δt, total power, and stem angle square root [31], [32]. All IMU data features were then saved into a single feature vector I. A full description of all features is provided as supplementary material.

3) Pressure Sensor + IMU Data: Pressure sensor and IMU features were combined in order to see whether the mechanically filtered combination of pressure sensor and IMU signals aided in improving HMU classification.

G. Feature Selection

To reduce the number and size of features based on high-dimensional data, it was necessary to perform feature selection before classification. The aim of the feature selection procedure was to find a smaller subset of relevant features with satisfactory classification accuracies to reduce the computational complexity. Furthermore, feature selection can help to prevent overfitting [33]. In this paper, three different stepwise feature selection methods were applied: linear regression, genetic algorithm, and a backward–forward neural network.

Stepwise linear regression is a widely used systematic feature selection method, which adds and removes features based on their statistical significance (evaluated by the F-statistic) [37]. The entrance tolerance was set to 0.08, and the exit tolerance was set to 0.1.

The stepwise genetic algorithm is an optimization technique inspired by natural selection [38], [39]. We used a mutual information-based genetic algorithm, following [37]. The initial population size was set as 200 times the feature count. Parents for the next generation were selected via tournament (size 2), and the elite count was set to 1. The stopping criteria were a maximum number of 100 generations, or until the change in the fitness value was less than 0.002.

A backward–forward stepwise neural network [25] was applied taking the HMU classification accuracy as the average of 100 runs. This was performed initially including all variables again after eliminating/adding a single variable. If the classification accuracy increased more than 2% after eliminating/adding the variable, it was removed/added to the model.

Once features had been selected, they were classified using an ANN as described in Section II-H.

H. HMU Classification

ANNs are nonlinear, data-driven, self-adaptive mathematical models inspired by biological neurons. In this paper, a 10–10 backpropagation network with soft max neurons in each layer and a cross-entropy loss function were used. A soft max transfer function was selected in both layers to avoid the vanishing gradient problem. Results of this paper were obtained by training the network using a scaled conjugate gradient algorithm. The net is maximally trained for 1000 epochs (the number of times the weights are updated), or until the performance goal of 0 is achieved. The ANN was tested 100 times, and the classification accuracy value assessed to reduce the ANN variability. In each run, a data set was randomly divided into three groups of training (70%), validation (15%), and testing (15%) data. A supervised training

TABLE III
HMU CLASSIFICATION ACCURACIES WITH ONE HYDROMAST (HYDROMAST 1) DATA

Variable reduction process	Pressure sensor data (accuracy/features)	IMU data (accuracy/features)	Pressure + IMU data (accuracy/features)
Full feature vector	**65.86%** **3** (PS1, PS2, PS9)	**69.40%** **20** (I1-I20)	**82.93%** **23** (PS1, PS2, PS9, I1-I20)
Stepwise linear model	**59.33%** **1** (PS1)	none	**89.13%** **2** (PS9, I6)
Stepwise genetic algorithm	**64.66%** **2** (PS1, PS2)	**81.13%** **6** (I1, I2, I5, I15, I16, I18)	**87.46%** **5** (PS1, I1, I15, I16, I18)
Stepwise neural network	**66.30%** **2** (PS1, PS9)*	**87.83%** **8** (I2, I3, I5, I7, I8, I14, I17, I18)*	**85.50%** **7** (PS2, I1, I2, I5, I7, I17, I19)*

*Removed features

algorithm was used where every input pattern is related with an output pattern in order to determine the optimal ANN weights. Validation data were used to check for overfitting, and the test data were used to establish model performance [28].

III. RESULTS

The hydromast HMU classification rates were obtained for one hydromast (1, 2, or 3), a pair (hydromasts 1 and 2, 1 and 3, and 2 and 3), and for the complete array of three hydromasts. The objective was to determine if HMUs could be characterized with a single hydromast or if the spatial diversity of turbulent flows required additional units. Furthermore, pressure sensor and IMU data were used for HMU classification first separately and then jointly to see if pressure and inertial hydrodynamic signals work best alone or together. All features used in the classification are presented in the supplementary material. The best performing results and their features compared to the full feature vector of all pressure and IMU data are presented in Table III.

The best classification accuracy with pressure only data was 66.3% using the stepwise neural network. It was found that for the three HMU (glide, rapid, and riffle) studied in our work, pressure-based features had the lowest classification accuracies and smallest number of features, indicating that pressure-based hydrodynamic signals may demand a larger number of inputs to allow accurate discrimination between different locations. The IMU signals provided better classification accuracies, with a classification accuracy 88%. Due to the difference in feature size, the performance difference between pressure and IMU features could also be explained by the higher number of features and not alone by the stem's physical interactions with the flow.

Overall, it was found that combined features after stepwise linear feature reduction had the best performance, increasing the site localization accuracy to 89%. Although our data set was limited to three HMUs, these results indicate that combined pressure and inertial hydrodynamic features can improve overall classification accuracy. Combined data set results also depended less on the variable reduction method than the IMU data. Although our study includes data from a single river at three test sites, it should be noted that the combined features performed better with single hydromasts, pairs of hydromasts, and the three hydromast array.

In Fig. 5, the mean HMU classification results are presented for 1, 2, and 3 hydromasts. It can be concluded that increasing the number of hydromasts improved the HMU classification accuracy. This was true in all cases expect one—the stepwise neural network, where the best result was obtained with a hydromast pair. However, it should be noted that the difference in classification accuracy was small; the corresponding average classification accuracy was 95.28% for two hydromasts and 93.33% for three hydromasts.

The relatively large standard deviation obtained with one hydromast while using linear regression method can be related to the feature selection criteria. In some cases, only a single feature was selected. It is possible that increasing the entrance tolerance in this case, when the feature set is relatively small, may lead to better results.

Overall, the best performance was obtained using three hydromasts and the linear regression method for ten features, with a classification accuracy 93.30%. Out of those ten features, six were pressure based (P3, P4, P25, P28, P29, and P32) and four were from the IMU data (I2, I15, I38, and I55). As shown in Fig. 5, it can be concluded that the choice of feature selection methods can impact the results, but has the least impact for an array of three hydromasts. Indeed, considering the classification performance of single or hydromast

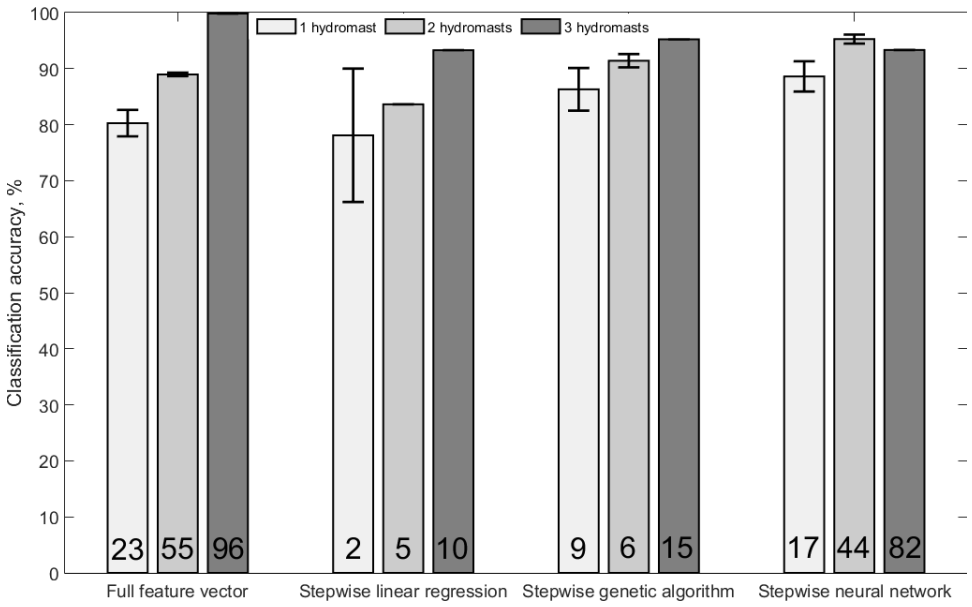

Fig. 5. Average HMU classification results with one, two, and three hydromasts. Values at the bottom of the bar plot represent the average number of features found by each method.

pairs, the results were found to depend more on the selected method than the choice of devices.

An HMU classification confusion plot for the hydromast array using the stepwise linear regression feature selection method is presented in Fig. 6. This feature set was selected as it provided an overall satisfactory classification accuracy when compared to the other methods, and included a low number of ten features.

Fig. 6 illustrates that all the locations from Sites 1 and 2 are classified correctly. However, the classification accuracy of Site 3 was 80%. The lower classification accuracy is caused by two locations in Site 3 which are incorrectly classified as Site 1. This may be due to the aforementioned physical similarity between sites. The HMU classification accuracy depended on the measurement length using ten features and is presented in Fig. 7.

It can be seen from Fig. 7 that the measurement time of 90 s could be increased in future studies, as convergence of the classification accuracy was not achieved for Sites 2 and 3. As expected, Site 1, in which flow conditions were the simplest, converged the fastest. The classification accuracy evolution of Site 2 was found to be more rapid than that of Site 3. This can be explained the unique flow patterns in Site 2 compared to other two sites. The classification accuracy of Site 3 converges more slowly because of its high similarity to Site 1.

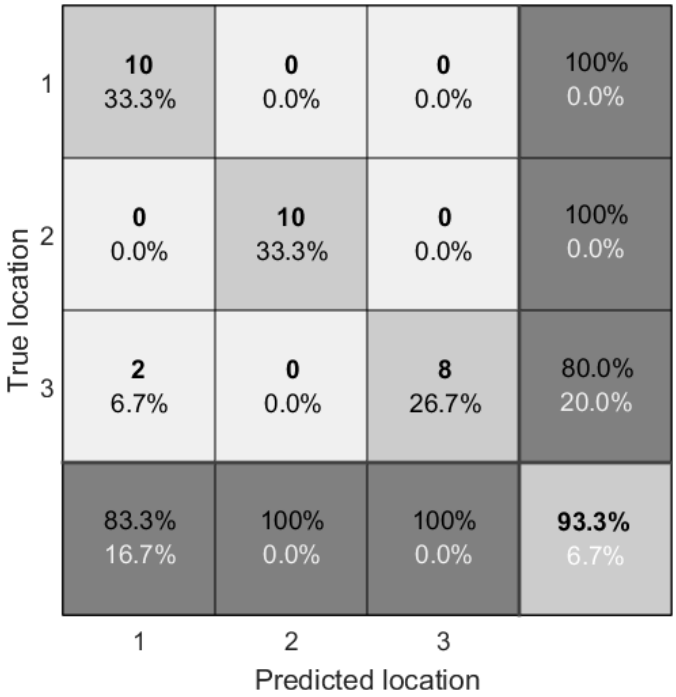

Fig. 6. Classification accuracies between all three sites using the stepwise linear regression feature selection method.

IV. Discussion

Classification of river HMUs and monitoring their changes can improve our understanding of how rivers change in time. For example, it has been shown that changes of river hydromorphology strongly impact fish and macroinvertebrates [38]. Monitoring changes of HMUs can aid in mitigating future risk, and planning improvements to hydromorphological quality [8], [39]. We believe that the hydromast, a portable and inexpensive device, offers a new method for simple field-based classification at the reach scale. Furthermore, long-term installations of hydromast networks could provide timesaving distributed monitoring currently not possible using acoustic Doppler devices.

It was shown that correct classification of the three different HMUs investigated can be achieved using only a vibrating stem. The IMU features provided a classification accuracy of 88% with only one hydromast (using stepwise neural net-

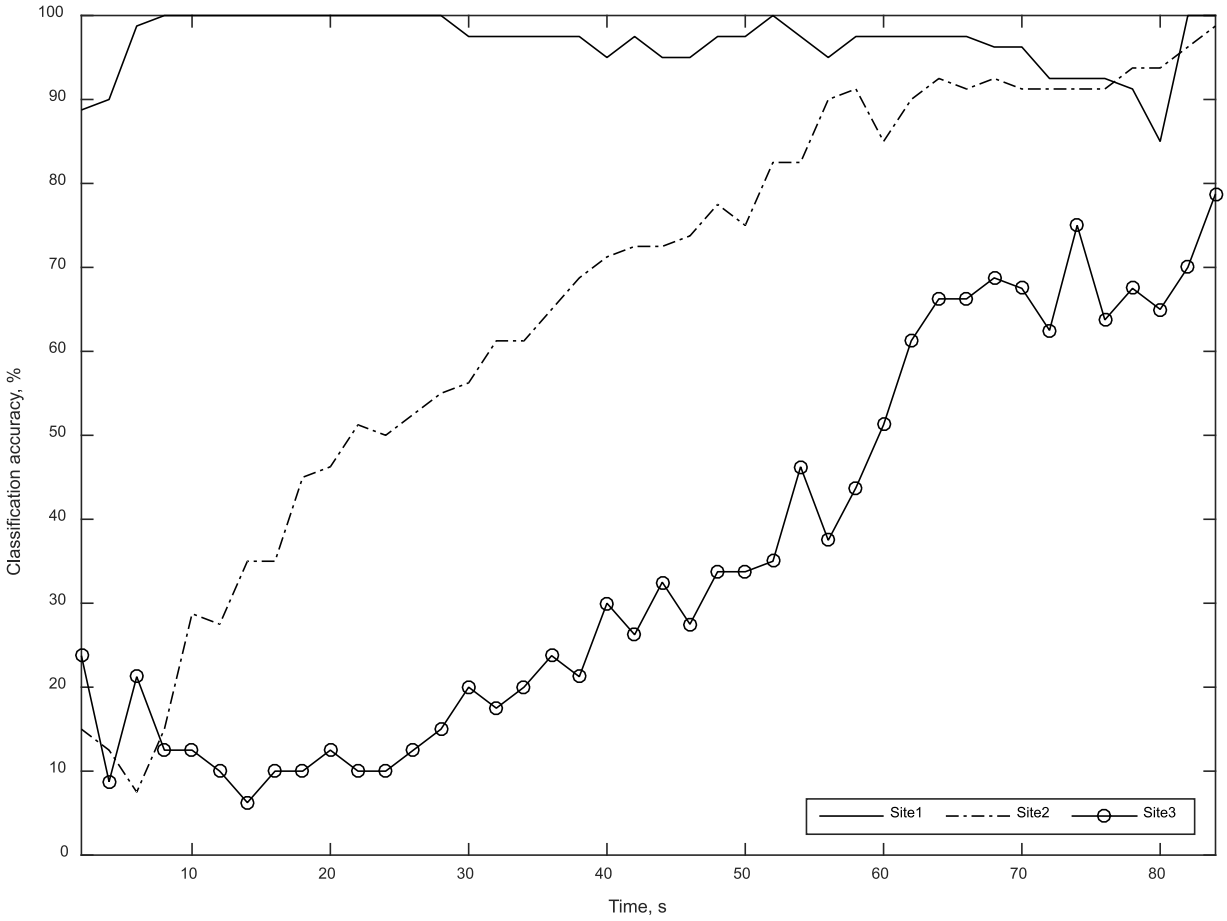

Fig. 7. Evolution of classification accuracies with increasing sampling duration.

work), and when including IMU features from two additional hydromasts, a classification accuracy of 93% was obtained (using stepwise neural network).

The accuracy of a single hydromast can be increased by including pressure sensor features (Table III). The pressure sensors detect localized, rapid changes in the flow (e.g., detect the water surface fluctuations and local pressure fluctuations due to vorticity). The stem picks up slower changes in the flow because of the vertically integrated forcing and vortex shedding, and its features can be insufficient to differentiate between HMUs where the time-averaged velocity and depths are similar. When combined pressure and IMU features using a triple hydromast array are used, a classification accuracy of 99% was reached (using full feature set).

We believe that both the device and the processing approaches can be implemented by nonexperts who would only need to be able to place the hydromasts in the river, collect the data, and run the data processing algorithms in order to perform HMU classification. It is our ultimate aim to have a data-driven workflow, which is completely independent of the operator, and provides unbiased data, which can be compared for any series of field measurements.

Due to the preliminary nature of the case studies investigated, a larger number of sites covering broader range of conditions are required to estimate baseline field assessment performance. In this paper, the high accuracy of site classification using IMU features must be considered as provisional, as the study included only a single set containing a glide, a rapid, and a riffle. In order to determine a more definitive understanding of the proposed method, it is important to investigate additional HMU types in multiple rivers under a range of flow conditions.

V. Conclusion

We developed and field-tested the hydromast, a multimodal sensor for HMU classification. A total of 30 locations were classified, ten in each of the three HMU sites. The sites were chosen due to their difficult classification using standard point-based methods; they were shallow and had highly turbulent flows with smooth and rough beds. We showed that the hydromast could successfully differentiate between three different river HMUs with a classification accuracy of 89% (using stepwise linear model). An array of three synchronized hydromasts provided increased classification accuracy of 93% after feature optimization (using stepwise linear model). The fluid–body interactions of the flow and hydromast allowed real-time mechanical filtering, simple signal processing, and feature extraction using an ANN. The field study results indicate that our approach provides a new methodology for rapid and robust natural flow classification of HMUs in rivers.

REFERENCES

[1] E. Muller, H. Décamps, and M. K. Dobson, "Contribution of space remote sensing to river studies," *Freshwater Biol.*, vol. 29, no. 2, pp. 301–312, Apr. 1993.

[2] I. P. Vaughan *et al.*, "Integrating ecology with hydromorphology: A priority for river science and management," *Aquatic Conservation Marine Freshwater Ecosyst.*, vol. 19, no. 1, pp. 113–125, Jan./Feb. 2009.

[3] X. Zhang, S. Wang, X. Liu, and W. Li, "Study on digital river basin information technologies and application," in *Proc. Int. Conf. Inf. Sci., Electron. Elect. Eng.*, vol. 2. Apr. 2014, pp. 949–953.

[4] L. Geng, M. Ma, and H. Wang, "An effective compound algorithm for reconstructing MODIS NDVI time series data and its validation based on ground measurements," *IEEE J. Sel. Topics Appl. Earth Observ. Remote Sens.*, vol. 9, no. 8, pp. 3588–3597, Aug. 2016.

[5] T. Moss, "The governance of land use in river basins: Prospects for overcoming problems of institutional interplay with the EU Water Framework Directive," *Land Policy*, vol. 21, no. 1, pp. 85–94, Jan. 2004.

[6] M. L. Ribeiro, K. Blanckaert, A. G. Roy, and A. J. Schleiss, "Hydromorphological implications of local tributary widening for river rehabilitation," *Water Resour. Res.*, vol. 48, no. 10, p. W10528, Oct. 2012.

[7] C. K. Feld, F. de Bello, and S. Dolédec, "Biodiversity of traits and species both show weak responses to hydromorphological alteration in lowland river macroinvertebrates," *Freshwater Biol.*, vol. 59, no. 2, pp. 233–248, Feb. 2014.

[8] M. Rinaldi, N. Surian, F. Comiti, and M. Bussettini, "A method for the assessment and analysis of the hydromorphological condition of Italian streams: The Morphological Quality Index (MQI)," *Geomorphology*, vols. 180–181, pp. 96–108, Jan. 2013.

[9] S. Bizzi, L. Demarchi, R. C. Grabowski, C. J. Weissteiner, and W. Van de Bund, "The use of remote sensing to characterise hydromorphological properties of European rivers," *Aquatic Sci.*, vol. 78, no. 1, pp. 57–70, Jan. 2016.

[10] P. Parasiewicz, "MesoHABSIM: A concept for application of instream flow models in river restoration planning," *Fisheries*, vol. 26, no. 9, pp. 6–13, Sep. 2001.

[11] A. M. Mouton, M. Schneider, J. Depestele, P. L. M. Goethals, and N. De Pauw, "Fish habitat modelling as a tool for river management," *Ecol. Eng.*, vol. 29, no. 3, pp. 305–315, Mar. 2007.

[12] C. C. Teague, D. E. Barrick, and P. M. Lilleboe, "Geometries for streamflow measurement using a UHF RiverSonde," in *Proc. IEEE Int. Geosci. Remote Sens. Symp. (IGARSS)*, vol. 7. Jul. 2003, pp. 15–17.

[13] C. C. Teague, D. E. Barrick, P. M. Lilleboe, and T. Ralph, "Two-dimensional surface river flow patterns measured with paired riversondes," in *Proc. Int. Geosci. Remote Sens. Symp.*, 2007, pp. 2491–2494.

[14] D. W. Dobson, K. T. Holland, and J. Calantoni, "Fast, large-scale, particle image velocimetry-based estimations of river surface velocity," *Comput. Geosci.*, vol. 70, pp. 35–43, Sep. 2014.

[15] F. Tauro, G. Olivieri, A. Petroselli, M. Porfiri, and S. Grimaldi, "Flow monitoring with a camera: A case study on a flood event in the Tiber River," *Environ. Monitor. Assessment*, vol. 188, no. 2, p. 118, Feb. 2016.

[16] I. Fujita, H. Watanabe, and R. Tsubaki, "Development of a non-intrusive and efficient flow monitoring technique: The space-time image velocimetry (STIV)," *Int. J. River Basin Manage.*, vol. 5, no. 2, pp. 105–114, 2007.

[17] C. Hauer, G. Mandlburger, and H. Habersack, "Hydraulically related hydro-morphological units: Description based on a new conceptual mesohabitat evaluation model (MEM) using LiDAR data as geometric input," *River Res. Appl.*, vol. 25, no. 1, pp. 29–47, Jan. 2009.

[18] W. Gostner, M. Alp, A. J. Schleiss, and C. T. Robinson, "The hydro-morphological index of diversity: A tool for describing habitat heterogeneity in river engineering projects," *Hydrobiologia*, vol. 712, no. 1, pp. 43–60, Jul. 2013.

[19] J. M. H. Cockburn, P. V. Villard, and C. Hutton, "Assessing instream habitat suitability and hydraulic signatures of geomorphic units in a reconstructed single thread meandering channel," *Ecohydrology*, vol. 9, no. 6, pp. 1094–1104, Sep. 2016.

[20] A. Mancini, E. Frontoni, P. Zingaretti, and S. Longhi, "High-resolution mapping of river and estuary areas by using unmanned aerial and surface platforms," in *Proc. Int. Conf. Unmanned Aircraft Syst. (ICUAS)*, Jun. 2015, pp. 534–542.

[21] E. Naudascher and D. Rockwell, *Flow-Induced Vibrations: An Engineering Guide*. North Chelmsford, MA, USA: Courier Corporation, 2012.

[22] A. Ristolainen, J. A. Tuhtan, A. Kuusik, and M. Kruusmaa, "Hydromast: A bioinspired flow sensor with accelerometers," in *Biomimetic and Biohybrid Systems*, vol. 8064, N. F. Lepora, A. Mura, H. G. Krapp, P. F. M. J. Verschure, and T. J. Prescott, Eds. Berlin, Germany: Springer, 2016, pp. 510–517.

[23] J. F. Fuentes-Pérez, K. Kalev, J. A. Tuhtan, and M. Kruusmaa, "Underwater vehicle speedometry using differential pressure sensors: Preliminary results," in *Proc. AUV*, Nov. 2016, p. 6.

[24] *Estonian Weather Service*. Accessed: Feb. 13, 2017. [Online]. Available: http://www.ilmateenistus.ee/?lang=en

[25] M. Haghighat, M. Abdel-Mottaleb, and W. Alhalabi, "Discriminant correlation analysis: Real-time feature level fusion for multimodal biometric recognition," *IEEE Trans. Inf. Forensics Security*, vol. 11, no. 9, pp. 1984–1996, Sep. 2016.

[26] A. K. Smilde, M. J. van der Werf, S. Bijlsma, B. J. C. van der Werff-van der Vat, and R. H. Jellema, "Fusion of mass spectrometry-based metabolomics data," *Anal. Chem.*, vol. 77, no. 20, pp. 6729–6736, 2005.

[27] A. Downey, "Think DSP," Tech. Rep., 2016.

[28] J. A. Tuhtan, J. F. Fuentes-Perez, G. Toming, and M. Kruusmaa, "Flow velocity estimation using a fish-shaped lateral line probe with product-moment correlation features and a neural network," *Flow Meas. Instrum.*, vol. 54, pp. 1–8, Apr. 2017.

[29] R. Telgàrsky. (2013). "Dominant frequency extraction." [Online]. Available: https://arxiv.org/abs/1306.0103

[30] C. Erbe, "Underwater acoustics: Noise and the effects on marine mammals," in *A Pocket Handbook*, vol. 164, 3rd ed. Halifax Regional Municipality, NS, Canada: JASCO Applied Sciences, Apr. 2011.

[31] W. H. Press, *Numerical Recipes 3rd Edition: The Art of Scientific Computing*. Cambridge, U.K.: Cambridge Univ. Press, 2007.

[32] L. Hoehn and I. Niven, "Averages on the Move," *Math. Mag.*, vol. 58, no. 3, p. 151, May 1985.

[33] J. Tang, S. Alelyani, and H. Liu, "Feature selection for classification: A review," in *Data Classification: Algorithms and Applications*. Boca Raton, FL, USA: CRC Press, 2014, pp. 37–64.

[34] N. R. Draper and H. Smith, "Applied regression analysis," *Technometrics*, vol. 47, no. 3, p. 706, 1998.

[35] M. Mitchell, "An introduction to genetic algorithms," *Sadhana*, vol. 24, nos. 4–5, pp. 293–315, Aug. 1999.

[36] D. Whitley, "A genetic algorithm tutorial," *Statist. Comput.*, vol. 4, no. 2, pp. 65–85, Jun. 1994.

[37] O. Ludwig and U. Nunes, "Novel maximum-margin training algorithms for supervised neural networks," *IEEE Trans. Neural Netw.*, vol. 21, no. 6, pp. 972–984, Jun. 2010.

[38] D. Hering, R. K. Johnson, S. Kramm, S. Schmutz, K. Szoszkiewicz, and P. F. M. Verdonschot, "Assessment of European streams with diatoms, macrophytes, macroinvertebrates and fish: A comparative metric-based analysis of organism response to stress," *Freshwater Biol.*, vol. 51, no. 9, pp. 1757–1785, Sep. 2006.

[39] A. M. Gurnell *et al.*, "A multi-scale hierarchical framework for developing understanding of river behaviour to support river management," *Aquatic Sci.*, vol. 78, no. 1, pp. 1–16, Jan. 2016.

Asko Ristolainen received the B.Sc. and M.Sc. degrees in mechatronics, and the Ph.D. degree in information and communication technology from the Tallinn University of Technology, Tallinn, Estonia, in 2008, 2010, and 2015, respectively.

He is currently a Researcher with the Centre for Biorobotics, School of Information Technologies, Tallinn University of Technology, where he involved in Lakhsmi Project. His research interests include environmental sensing, flow sensor design, and mechanics.

Kaia Kalev received the B.Sc. degree in engineering physics from the Tallinn University of Technology, Tallinn, Estonia, in 2014, and the M.Sc. degree in joint study curriculum biomedical engineering and medical physics from the Tallinn University of Technology and Tartu University, Tartu, Estonia, in 2016. She is currently pursuing the Ph.D. degree with the Centre for Biorobotics, School of Information Technologies, Tallinn University of Technology.

She is currently a Junior Researcher with the Centre for Biorobotics, School of Information Technologies, Tallinn University of Technology. Her research interests include environmental sensing and signal processing.

Jeffrey Andrew Tuhtan received the B.Sc. degree in civil engineering with California Polytechnic University, San Luis Obispo, CA, USA, in 2004, and the M.Sc. degree in water resources engineering and management and the Dr.-Eng. degree in hydraulics from the University of Stuttgart, Stuttgart, Germany, in 2007 and 2011, respectively.

He is currently with the Centre for Biorobotics, Department of Computer Systems, Tallinn University of Technology, Tallinn, Estonia, where he leads the Environmental Sensing and Intelligence Group. His research interests include environmental intelligence, applied fluid mechanics, and remote sensing.

Alar Kuusik received the Ph.D. degree in IT from the Tallinn University of Technology, Tallinn, Estonia, in 2001.

He is currently a Senior Researcher with the Thomas Johann Seebeck Department of Electronics, Tallinn University of Technology. He participated several internship programs in Germany, Japan, Sweden, and USA. His research interests include Internet of Things sensing and connectivity technologies and applications.

Maarja Kruusmaa is the Head of the Centre for Biorobotics, Tallinn University of Technology, Tallinn, Estonia. Her research interests include flow sensing, underwater robots, bioinspired robot locomotion, experimental fluid dynamics, and robot learning.